# Aspects of the photometric G band calibration and the expected photometric precision


**H. Voss , C. Jordi, C. Fabricius, F. Figueras, J.M. Carrasco, M. Gebran**

*Universitat de Barcelona, ICC-IEEC, Martí i Franqués, 1, 08028 Barcelona, Spain*

UNIVERSITAT DE BARCELONA

Institut de Ciències del Cosmos

For more information please contact H. Voss (hvoss@am.ub.es)



# Abstract

***Gaia*** **will observe about 1 billion sources at about 80 different epochs on the average providing broad-band white-light photometry (G band). The instrumental sensitivity depends on many different effects that will also change with time. The *Gaia* instrument is a rather complex device. Each of the 62 CCDs used for G band observations will show its own sensitivity behaviour depending on wavelength, the across scan position of the observation and time. The PSF will vary across the two FoVs. A fraction of the total flux will not be recorded due to the discrete size of the apertures. Non-linearity of the CCDs, residuals of the CTI-effects, sensitivity variations originating from the optics and the variations mentioned before have to be internally calibrated for all of the different instrument configurations (gates, 2D windows, 1D windows, ...). This internal calibration aims to transfer all the single observations by different instrumental configurations to observations as made by a mean instrument. In a second step this flux data has to be calibrated externally providing 'true' fluxes.**

**The CU5 group is responsible for developing and executing the rather complex calibration process for the G band photometry. The team of the University of Barcelona has investigated single effects like sensitivity variations on CCD and CCD column level, non-linearities, flux loss due to the limited sized of the extraction windows and combinations of these effects. All known effects affecting the G band observations will have to be taken into account when the tests of different calibration models are continued.**

**Based on the calibration tests already carried out preliminary expected errors of the photometric precision for the G band will be provided allowing a better evaluation of what kind of scientific results can be derived from *Gaia* G band photometry.**


# Calibration Scheme

**Proposed scheme of the Internal Calibration of the G band:**

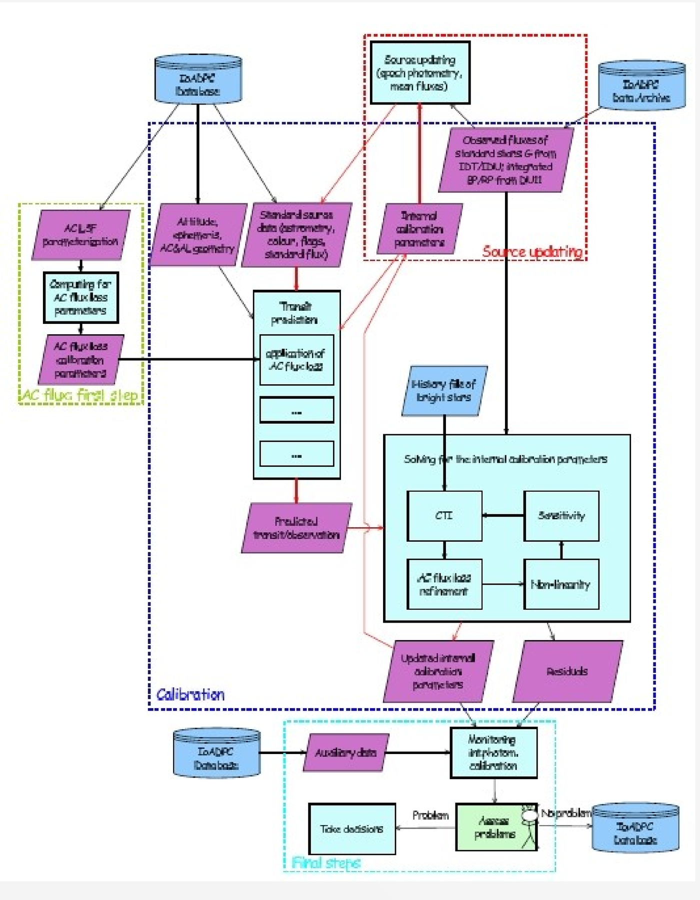

The aim of the internal calibration is to provide an internally consistent flux scale for the entire mission duration. As the Gaia instrument is a rather complex device with 62 CCDs in the FPA, 2 FoVs, gated and ungated observations with different window classes which will observe about 1 billion sources this is a very challenging task.

The standard principle of the calibration procedure is to derive standard fluxes from the Gaia observations themselves and take these observations in combination with the current set of calibration parameters to make a prediction of the observed fluxes to derive a new set of the internal calibration parameters. The instrumental variations can be be described as small corrections to the current set of calibration parameters.

The data is assumed to be **preprocessed** (basic image calibration, bias and background subtracted, CTI (Charge Transfer Inefficiencies) effects estimated).

**The internal calibration includes:**

- **Selection** of a large set of suitable **reference sources** (non-variable, isolated, distribution in colour, space and time)
- Prediction of the **across scan flux loss** for 1D window observations based on the current PSF/LSF model
- The iterative solution itself solves for a new set of calibration parameters based on the predicted observations and takes care of **sensitivity variations** of the instrument on different scales, **non-linearities** of the CCDs and **residuals of CTI and across flux loss.**
- **Monitoring of the residuals** to discover any new change of the instrument which is not covered yet by the calibration model currently used.

The aim is to reach a precision of the internal calibration which is limited by the observational noise and not by the calibration noise. **The calibration noise should at least be five times smaller than the observational noise.**

Additionally an external flux calibration has to be applied to connect the internally calibrated Gaia data with the real world comparing the fluxes of SPSS (**S**pectro-**P**hotometric **S**tandard **S**tars) which are observed spectrophotometrically from the ground.

# Across-scan flux loss

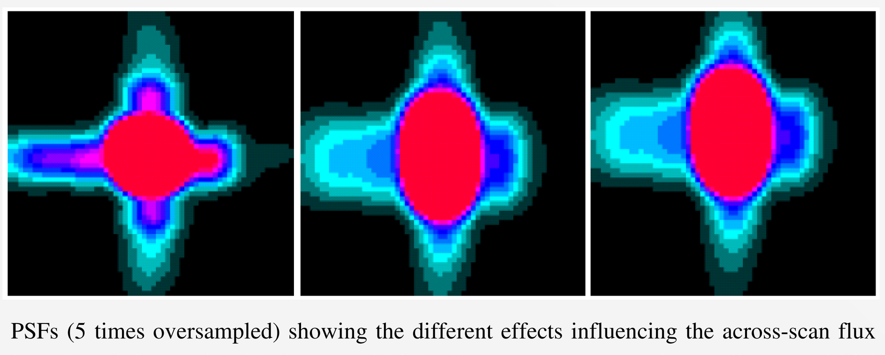

PSFs (5 times oversampled) showing the different effects influencing the across-scan flux loss (from left to right): Well-centered PSF with no across scan motion, well-centered PSF with nominal (mean) across scan motion and PSF decentered by one Gaia pixel with nominal across scan motion. Note that the PSFs are also varying with the colour of the source and the position in the FoV.

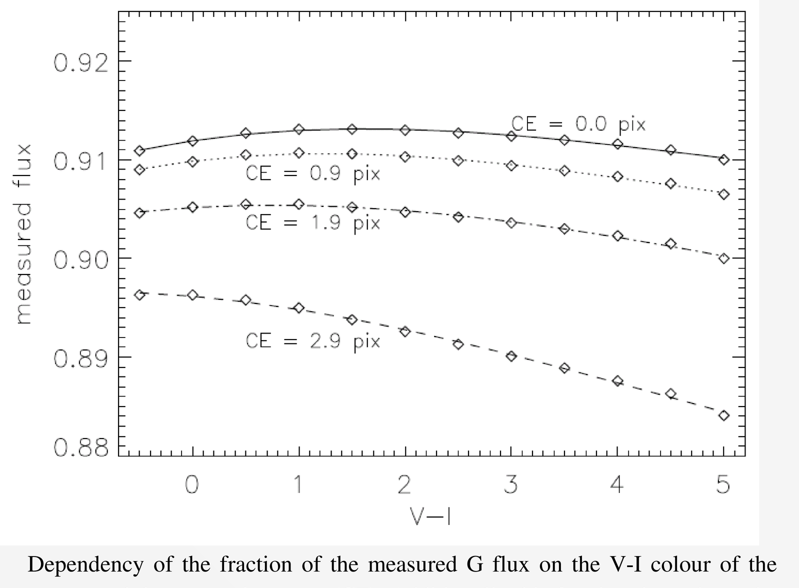


Dependency of the fraction of the measured G flux on the V-I colour of the source and the centering error (CE). Additionally this fraction depends on the scan motion of the satellite.

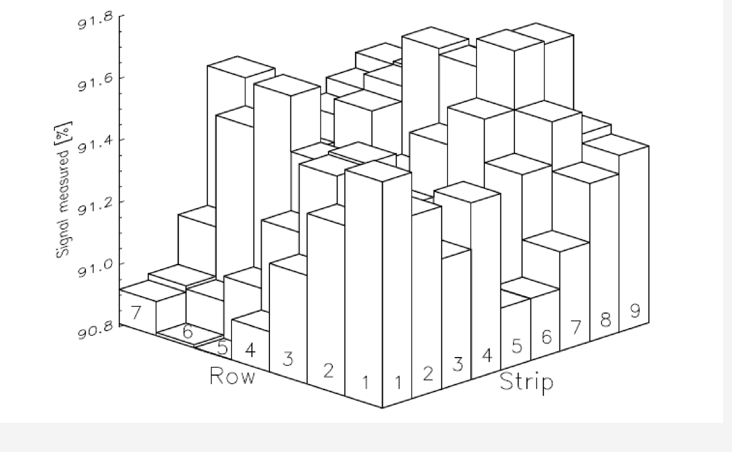


Variation of the measured signal within the 12 x 12 pixel extraction window for typical PSFs in the centre of the CCDs in FoV 1 with no across scan motion and perfect centering. Note the large variations from CCD-to-CCD in some areas of the FoV. The range of the across-scan flux loss is widened to about 2.7% also considering different across scan motions, centering errors and colours of the sources.

Due to the limited size of the extraction window not all light from the sources reaching the focal plane is converted into a measured signal. A fraction of about **10% of the signal is lost outside the window** depending on the **colour** of the source, the **centering error** (CE) of the PSF within the window, the **across scan motion** of the satellite and the position of the source within the FoV. For 2D observations this flux loss can be corrected by fitting PSF/LSF fitting. For 1D observations (G>13) without recorded across component only the flux loss along scan can be estimated by LSF fitting.

The across-scan flux loss was analysed in dependence on source colour (-0.5<V-I<5.0), CE ((-2.9<CE<+2.9) pixel), across scan motion (zero to maximal) and position in the FoV using simulated PSFs for the centre of the CCD/FoV combinations. **The variation of the flux loss with a range of up to 2.7%** is significant and is accounted for in the internal calibration.

# Sensitivity variations

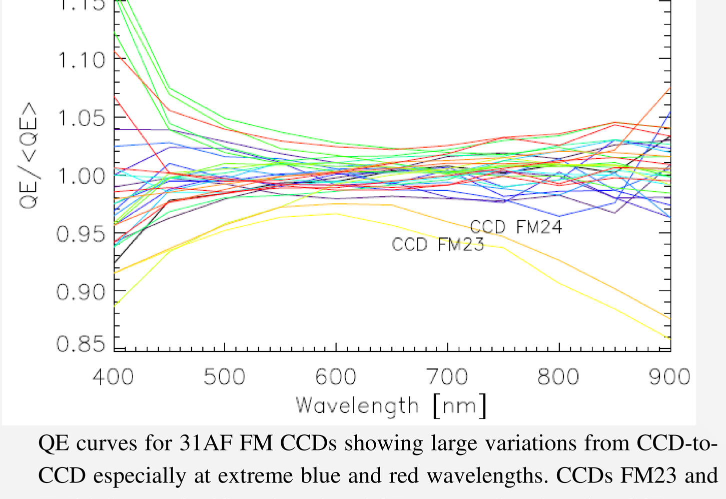


QE curves for 31AF FM CCDs showing large variations from CCD-to-CCD especially at extreme blue and red wavelengths. CCDs FM23 and FM24 show a significantly reduced QE compared to the other CCDs.

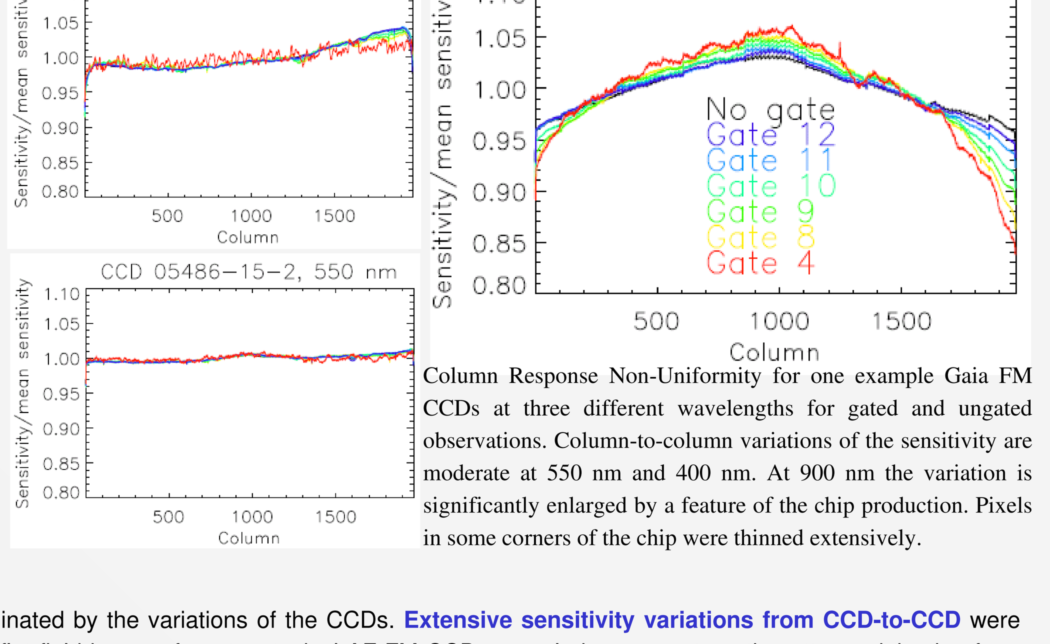


Column Response Non-Uniformity for one example Gaia FM CCDs at three different wavelengths for gated and ungated observations. Column-to-column variations of the sensitivity are moderate at 550 nm and 400 nm. At 900 nm the variation is significantly enlarged by a feature of the chip production. Pixels in some corners of the chip were thinned extensively.

The sensitivity variations of the instrument are thought to be dominated by the variations of the CCDs. **Extensive sensitivity variations from CCD-to-CCD** were found especially at extreme red and blue wavelengths. Analysing flat field images from two typical AF FM CCDs revealed some systematic pattern originating from the annealing process during the donation procedure of the chips. As the Gaia CCDs will work in TDI mode the combined sensitivity of a full column (or parts of it for gated observations of bright sources) is relevant. Thus this systematic pattern is only important for observations with the shortest gates activated. At intermediate wavelengths **the column-to-column sensitivity variations** are small for gated and ungated observations. A feature of the Gaia AF CCD chips is that two corners and the corresponding edge are extensively thinned (**corner effect**). At red wavelengths (where the sensitivity directly scales with the pixel thickness; Ralf Kohley, private communication) this yields to a reduced sensitivity of up to 40% compared to the other areas of the CCD on the pixel level. On the column-to-column level this effect is smaller. Depending on the two possible orientations of the chip during the thinning process it affects more the short gated observation (variation across > 20%) or the ungated observations (variations across > 8%). This effect is thought to complicate especially the calibration of red sources which are rare in relative numbers and often variable.

Image below: Flatfields for two example Gaia FM CCDs.

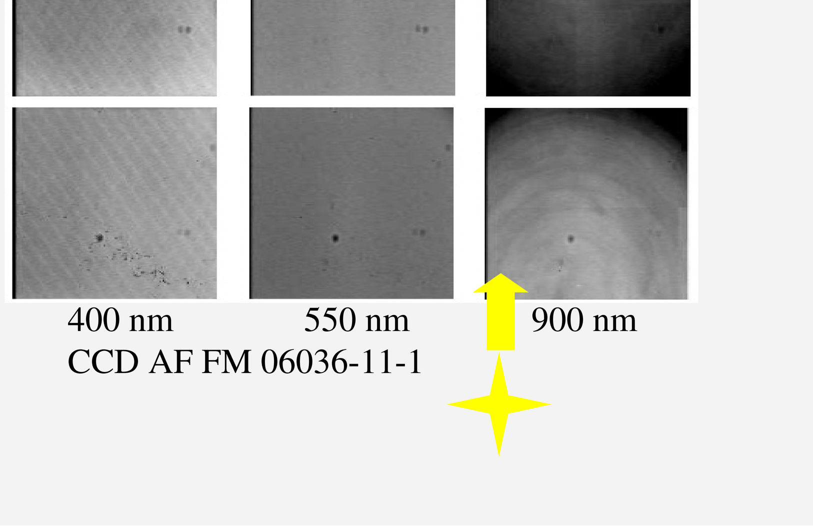


The sensitivities of the CCDs, their columns and the entire instrument is also expected to vary with time mainly due to radiation damage on the pixel level. Based on information about other space missions (HST STIS & ACS, XMM OM) with comparable instrument units the effect is thought to be in an order or less than 1% per year of mission time. The effect will be wavelength-dependent, blue wavelengths are more affected than red wavelengths.

The **reflectivity of the optical elements** will decline moderately by out-gassing and contamination with dust particles originating from the outer-space environment.

# Expected photometric precision

The aim is that the total noise after internal calibration is not dominated by the calibration noise but by the observation noise. This can be achieved by **setting an upper limit for the calibration noise to 20% of the observation noise.** As it was shown in calibration tests the derived calibration results are still below this limit. Nevertheless, as the simulated data did not contain all known effects (e.g.. CTI, non-linearities), it is still uncertain if this level of photometric precision can be really obtained for real Gaia data.

Following an aperture photometry approach the observation noise itself is computed based on the latest information about the total detection noise per pixel/sample and the sky background noise per pixel/sample. The mean number of observations is assumed to be 80. The flux lost outside the extraction window was estimated to 0.1 of the total flux. The different effective exposure times were taken into account for gated observations. 2D windows were assumed for all sources with G < 13 for the G band observations. For BP and RP band observations this limit was set to G < 11. The different window classes are based on the latest information available. No saturation effects are accounted for. An extra-margin of 20% accounting for the calibration noise has been added.

**From this computation, the estimated end-of-mission photometric precision is shown in the figure to the right.** G and integrated $G_{BP}$ and $G_{RP}$ yield uncertainties at mmag level or better.

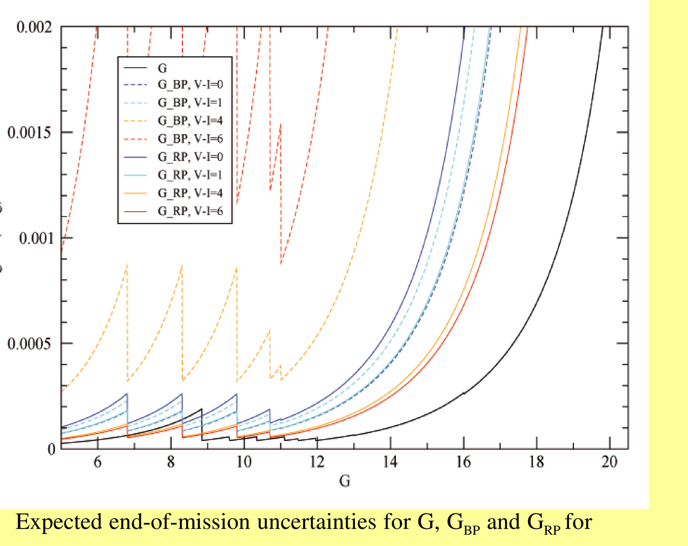


Expected end-of-mission uncertainties for G, $G_{BP}$ and $G_{RP}$ for sources with the colours V-I=0, 1, 4 and 6. $G_{BP}$ and $G_{RP}$ are the integrated flux of the BP and RP spectra.

# Calibration tests with simulated data

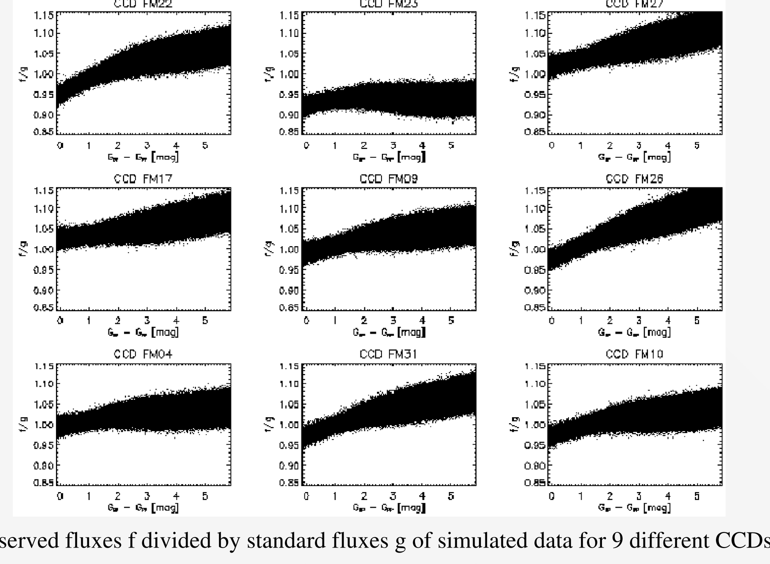


Observed fluxes f divided by standard fluxes g of simulated data for 9 different CCDs versus colour $G_{BP}$-$G_{RP}$. Note the variations especially for very red sources.

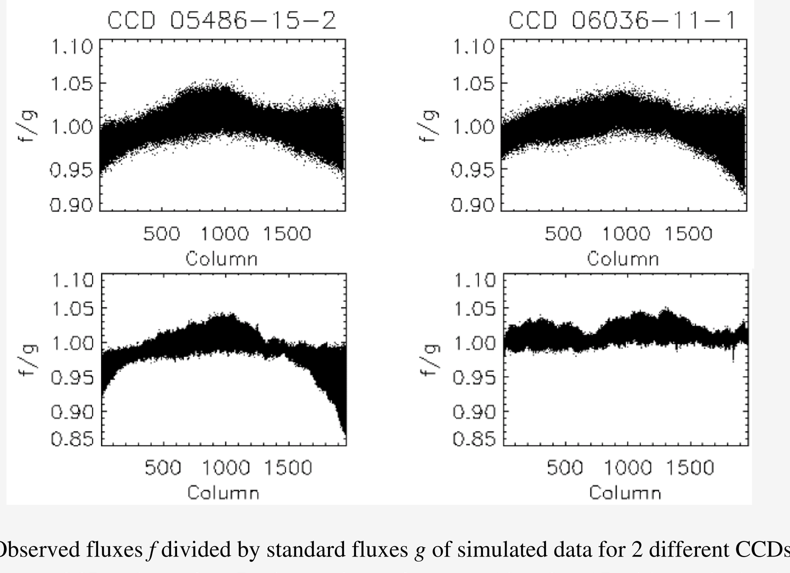


Observed fluxes *f* divided by standard fluxes *g* of simulated data for 2 different CCDs versus CCD column for 1D observations of sources 13 < G < 17 with nominal noise (upper part) and observations with the shortest gate #4 (low part).

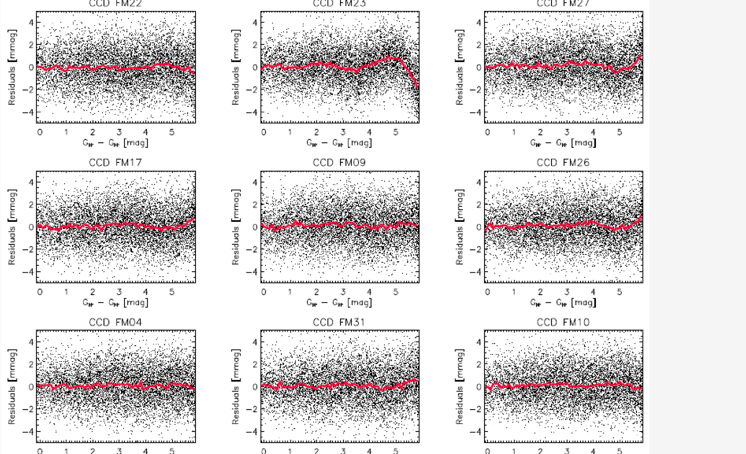

Residuals of the brightest sources after the calibration for the data of the 9 simulated CCDs vs. source colour . Note the large calibration residuals of red sources for some of the CCDs. The CCD-to-CCD sensitivity variations are dominating the residuals.

Based on the information from the industry a perfect data sample (uniform distributions in magnitude and colour) was simulated as observed by 9 representative Gaia FM CCDs. Realistic CCD-to-CCD (large scale) and column-to-column (small scale) sensitivity variations were included. The small scale variations were merged with a typical PSF to simulate the PSF smearing of the signal.

Sensitivity calibration tests were performed using different kinds of calibration models. The **general principle of the calibration models** is to use some simple spectrophotometric information of different degrees of complexity to be able to calibrate wavelength dependent effects:

$$f_l = \sum_{m=0}^{M} (A_{km} + a_{\kappa m}) g_{im}$$

Therein are:

$g_{im}$ - the standard fluxes of the source *i* in the photometric band *m*,

$A_{km}$ - the current large scale calibration coefficients for the calibration unit *k*,

$a_{\kappa m}$ - the small scale calibration coefficients for the calibration units *κ*.

They are used to derive a prediction for the observed fluxes $f_l$ of the observation *l*. The comparison of the observed fluxes and the predictions allows to refine stepwise the large and small scale calibration coefficients.

The calibration tests included passband information in the form of easily accessible Gaia data: G, $G_{BP}$ and $G_{RP}$ fluxes and combinations of them. The different calibration models were tested if they allow to derive sufficient results for our simulated data with the rather complex dependencies on wavelength for the sensitivity variations. Only one model was found to be able to produce sufficient results. This **model III uses the G band information and the flux difference terms of $G_{BP}$ - $G_{RP}$ up to fifth order**. In this way 6 small scale and 6 large scale calibration coefficients are derived for each calibration unit.

The analysis of the calibration residuals reveals that especially **for red sources some large residuals and systematic trends (up to 1 mmag)** are present for some CCDs. This is due to the large CCD-to-CCD sensitivity variations for red wavelengths. Note that for this simulated perfect data the calibration noise is below the 20% level of the observational noise even for red sources (also valid for gated observations). This is thought to change for more realistic data with different distribution in colour and magnitude and different effects like across-scan flux loss and non-linearities. Therefore some ways to improve the calibration were analysed. A simple solution is to limit the sensitivity calibration space by **replacing some CCDs with extreme QE curves by CCDs with more common QE curves**. As there will be some spare AF CCDs this seems to be a good possibility. Furthermore it seems unavoidable to use **more complex colour information for a better description** of the spectral energy distribution of the sources.

Unit-weight standard deviation vs. source colour for the calibrated data of CCD FM22 (black) and CCD FM23 (red) representing the best and the worst case of the calibration model. Note that the additional noise due to the calibration is well below 20% even for the worst case. CCD FM22 is one of the CCDs that eventually will be rejected from FM.

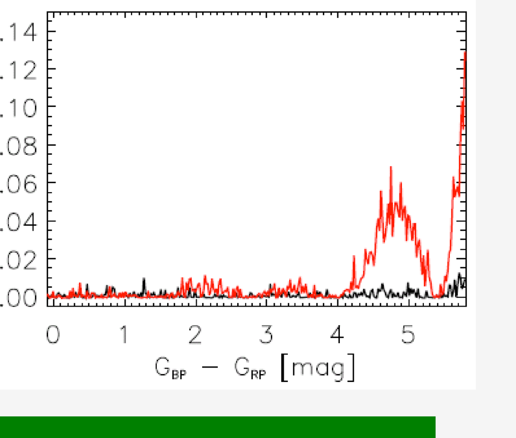


# Further aspects of the internal calibration

**Saturation:** In TDI mode the saturation can appear on pixel level, on column level and on the level of the summing and readout register. A first saturation can occur when the collected charge of a source is reaching the pixel with the lowest full-well-capacity (FWC) in the column. Additional saturation can occur further in the same column as more charge can be collected. Nevertheless, it is expected that the transition from saturation to the linear response is more or less smooth, but different for each column and CCD. Thus it will happen that some sources cause saturation in only some few CCDs. Intercomparison of the fluxes between the CCDs and between gated and ungated observations can be used to predict the signal loss in the saturated observations.

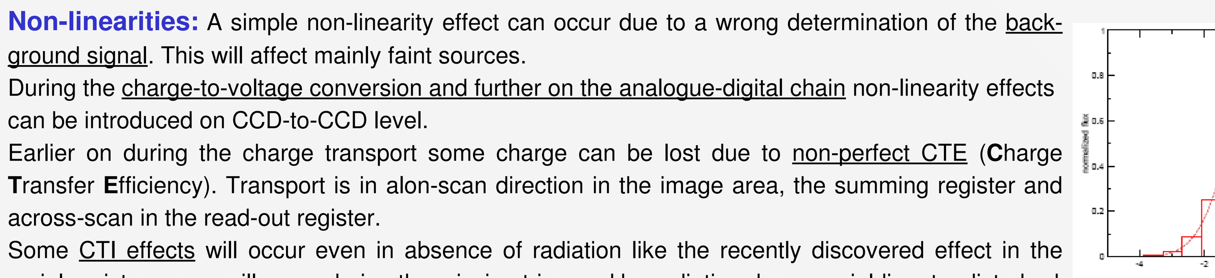

Example of the different full-well-capacity (FWC) of pixels for a typical Gaia CCD. Some large differences are visible at the boundaries of the stitches used during CCD chip production. Note that the FWC will also vary with time.

**Non-linearities:** A simple non-linearity effect can occur due to a wrong determination of the back-ground signal. This will affect mainly faint sources.

During the charge-to-voltage conversion and further on the analogue-digital chain non-linearity effects can be introduced on CCD-to-CCD level.

Earlier on during the charge transport some charge can be lost due to non-perfect CTE (**C**harge **T**ransfer **E**fficiency). Transport is in alon-scan direction in the image area, the summing register and across-scan in the read-out register.

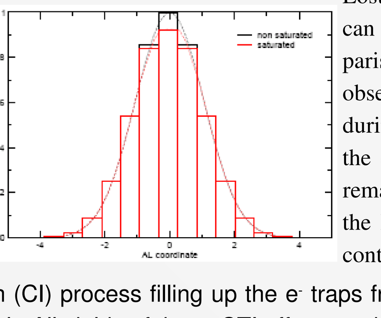


Lost signal due to saturation can be recovered by comparison of predicted with observed shape of an image during the preprocessing of the data. Some residuals will remain due to uncertainties of the PSF model and the noise content of the data itself.

Some CTI effects will occur even in absence of radiation like the recently discovered effect in the serial register, some will occur during the mission triggered by radiation damage yielding to disturbed PSFs and additional flux loss. The along scan CTI effect will be mitigated by a periodic **C**harge **I**njection (CI) process filling up the $e^-$ traps from time to time. Some residual CTI effects will remain depending on the history of transits, CI and radiation damage on pixel level. All yields of these CTI effects and its residuals have to be mitigated in the preprocessing of the data. Distorted PSFs/LSFs will be compared with predicted ones based on the information from the PSF/LSF model. Adjusting the model parameters by fitting the data allows to recreate a more or less undistorted signal. Due to uncertainties of the PSF/LSF model, noisiness of the data and computational restraints some residuals will be left to dealt within the internal calibration. As the current knowledge about these effects is partially still limited and no qualitative information about the expected residuals is available yet only basic ideas about the mitigation strategy within the internal calibration are under consideration at the moment. These strategies will be a main part of our future work.

**Polarization:** Intensity variations up to 1% are expected for bright, extremely polarized sources. As these sources are very rare the effect can be analyzed in the final solutions only.